Geomorphology 301 (2018) 21–27

Contents lists available at ScienceDirect

Geomorphology

journal homepage: www.elsevier.com/locate/geomorph

Predicting soil formation on the basis of transport-limited chemical weathering

Fang Yu [a,*], Allen Gerhard Hunt [a,b]

[a] Department of Earth & Environmental Science, Wright State University, 3640 Colonel Glenn Highway, Dayton, OH, United States
[b] Department of Physics, Wright State University, 3640 Colonel Glenn Highway, Dayton, OH, United States

ARTICLE INFO

Article history:
Received 23 March 2017
Received in revised form 25 October 2017
Accepted 30 October 2017
Available online 3 November 2017

Keywords:
Soil production
Soil formation
Chemical weathering
Percolation theory

ABSTRACT

Soil production is closely related to chemical weathering. It has been shown that, under the assumption that chemical weathering is limited by solute transport, the process of soil production is predictable. However, solute transport in soil cannot be described by Gaussian transport. In this paper, we propose an approach based on percolation theory describing non-Gaussian transport of solute to predict soil formation (the net production of soil) by considering both soil production from chemical weathering and removal of soil from erosion. Our prediction shows agreement with observed soil depths in the field. Theoretical soil formation rates are also compared with published rates predicted using soil age-profile thickness (SAST) method. Our formulation can be incorporated directly into landscape evolution models on a point-to-point basis as long as such models account for surface water routing associated with overland flow. Further, our treatment can be scaled-up to address complications associated with continental-scale applications, including those from climate change, such as changes in vegetation, or surface flow organization. The ability to predict soil formation rates has implications for understanding Earth's climate system on account of the relationship to chemical weathering of silicate minerals with the associated drawdown of atmospheric carbon, but it is also important in geomorphology for understanding landscape evolution, including for example, the shapes of hillslopes, and the net transport of sediments to sedimentary basins.

1. Introduction

As a complicated natural process (Vladychenskiy, 2009), soil formation is affected by five soil-forming factors: climate, topography, parent materials, organisms and time (Jenny, 1941; Dokuchaev, 1967). Defining soil formation as a continuous process helps to understand how soil and landscapes have developed and how they would be affected by climate change. Attempts to describe soil production have met with variable success. Soil depths tend to increase over time, but not in a linear fashion (Huggett, 1998), and not uniformly (data from the Heimsath references, i.e., Heimsath et al., 1997, 1999, 2001a, 2001b, 2005, 2009). In the main, soil depths increase more slowly the deeper is the soil.

Weathering of bedrock and erosion are two major processes affecting soil depth. Weathering is the slow process of disintegrating rocks to produce materials to form soil while erosion is transporting the loosened materials away, reducing soil depth. The details of the erosion process determine whether soil depth is lowered at any given site; whenever the divergence of the soil flux is positive, there is net transport of soil away from a point. The depth is reduced if the net transport off-site is greater than the soil production on site. The focus of the present paper is not on the details of the soil transport, merely on the effects of the net soil transport on the soil depth. The existence of soil implies that, locally, conditions are more favorable to weathering than to erosion (Anderson and Anderson, 2010), a situation termed transport-limited erosion (Carson and Kirkby, 1972). Since sediment transport is strongly relief-dependent (Montgomery and Brandon, 2002), one should expect small erosion rates, thus thicker soils, in regions of low relief.

Different analytical models describing soil production have been proposed, the exponential decay (Heimsath et al., 1997) of soil production with depth is almost universally applied. However, there are several reasons to prefer a power-law formulation. The most important is probably the proposed and observed correlation between soil production and chemical weathering rates as functions of time and depth (Burke et al., 2007; Dixon et al., 2009; Egli et al., 2014; Hunt and Ghanbarian, 2016). The importance of this correlation lies in the demonstrated (White and Brantley, 2003) power-law dependence of chemical weathering over time scales up to 6 Myr, which greatly exceeds the typical range of time scales addressed in most of the Heimsath references, thus clarifying the actual time-dependence. Further, Hunt and Ghanbarian (2016) also showed that the results of Friend (1992) and of Egli et al. (2014) for soil production rates were consistent with the same power-law form decay as chemical weathering rates, but to even larger timescales.

Based on previous work in modeling the production of soil using a simple power law that is derived from percolation theory (Hunt and Ghanbarian, 2016), here we propose a model to describe the formation

* Corresponding author.
E-mail addresses: yu.39@wright.edu (F. Yu), allen.hunt@wright.edu (A.G. Hunt).

https://doi.org/10.1016/j.geomorph.2017.10.027
0169-555X/

of soil. To avoid any confusion due to the existence of interchangeable concepts of "soil production" and "soil formation", in this paper, the term "soil production" refers to gross soil produced from the conversion of bedrock, while "soil formation" refers to the net effect by considering the removal of soil by erosion.

As proposed by Hunt and Ghanbarian (2016), soil production rate diminishes with a power of −0.47 with time (or a decay power of −0.87 with soil depth), and it is proportional to the deep infiltration rate in the field. Such a model involves the direct relevance of two soil-forming factors: climate and time, and possible indirect relevance of topography in affecting local climate and hydraulic condition. The model of soil formation presented in this paper will take the erosion (which itself is highly affected by topography) of soil into account. There are two other soil-forming factors left when discussing soil formation: parent materials and organisms. Effects from organisms, other than their contribution of CO_2 through respiration, on soil formation are beyond the scope of this research. Besides the composition of soil resulting from parent materials, what is more of concern in modeling soil formation is probably the effects of parent rocks on production rate. The soil production function this work is based on assumed weathering of (typically fractured) bedrock or regolith is solute transport-limited, so that the production of soil can be modeled without considering how resistant the parent materials are to weathering, since the production rate only depends on solute transport. The question of when weathering rates are limited by solute transport is usually addressed using the Damköhler number, Da_I, which is the ratio of a solute advection time to a reaction time. When $Da_I > 1$, transport limitations are considered relevant. Previous work studying Damköhler number (Yu and Hunt, 2017a) shows that over timescales exceeding days chemical weathering is practically always limited by transport. The solute transport limitations arise primarily from the diminishing solute velocity over time, which decays according to a power law. An additional factor is that fluid flow rates in nature are typically orders of magnitude slower than those investigated in laboratory experiments. Each of these inputs increases time scales associated with solute advection compared to what is often inferred, and guarantee that, over time, solute transport limitations to removing weathering products exceed the limitations from the kinetics of the weathering reaction.

Our approach is based on a network picture of the medium, in which percolation concepts can deliver the statistics and topologies of the dominant flow paths, including preferential flow. In accord with this hypothesis, we use percolation exponents to describe the tortuosity of such paths. Herein lie both similarities and differences to the approach of Lin (2010), which also addresses the influences of dominant flow paths over soil networks. In contrast to Lin's conjecture, we do not incorporate concepts of an evolution of the soil network to a state of higher organization and lower entropy, thus higher flow and solute transport rates. In the constructal law analogy invoked by Lin, one should expect an evolution towards more rapid flow and transport, with, e.g., smaller tortuosity of the flow paths. While very specific evidence for such evolution does indeed exist in river networks (which have values consistent with constructal theory at continental scales, rather than percolation theory values at all smaller scales (Hunt and Yu, 2017), our exploration has not yet revealed such relevance at soil scales. In fact, the reverse seems to occur. Vegetation seems rather to adapt to soil networks in such a way that their roots exploit existing optimal paths of percolation theory (Hunt, 2016, 2017).

We should also mention that the "energy" formulation of Runge (1973) bears some resemblance to ours. Runge's conceptual development also relates to Douchaev's soil formation factors, but, like ours, emphasizes the importance of vertical water flow. In our formulation, based on chemical weathering, the organisms supply the CO_2 for the weathering process, and the water flow rate, together with the pore separation (particle size) sets the fundamental time scale in the equation. This emphasis on water flow rates, which brings in climate (precipitation), vegetation (less evapotranspiration) plus topography (plus run-on less run-off) echoes the energy theory of Runge (1973), as discussed by Schaetzl and Schwenner (2006).

Finally, in conformance with the general perspective of Banwart et al. (2011), our discussion of the relevance of erosion then compares with our modern understanding of the importance of soil loss due to human activities generally. Banwart et al. (2011) note that soil erosion has increased by nearly a factor 100 due to various human endeavors. As will be seen below, such an increase in erosion rates leads, in our predictions, to a decrease in steady-state soil thickness by a factor $100^{1.14} = 191$, which would make soils everywhere useless for any usual human requirements.

2. Theoretical basis

Non-Gaussian (or non-Fickian) transport is becoming recognized as the norm in natural porous media (e.g., Cushman and O' Malley, 2015). Like Common descriptions of non-Gaussian transport such as Continuous Time Random Walk (CTRW) (Margolin and Berkowitz, 2000; Berkowitz et al., 2002; Bijeljic et al., 2004) or Fractional Advection Dispersion Equation (FADE) (Meerschaert et al., 1999; Benson et al., 2000; Pachepsky et al., 2000; Krepysheva et al., 2006), both of which model power-law solute arrival time distributions, percolation theory generates fat-tailed arrival time distributions, of approximately power-law form. However in contrast to both of these techniques, percolation theory does not yield an arbitrary power, the power-law arrival time distributions relate to the fractal dimensionality of the percolation backbone (Lee et al., 1999; Sheppard et al., 1999; Hunt and Skinner, 2008, 2010; Hunt et al., 2011; Ghanbarian-Alavijeh et al., 2012), making predictions of the actual power possible. Ability to predict this power in solute transport confers the ability to predict the power in the power-law of soil production.

The solute transport theory was first developed in Hunt and Skinner (2008) by applying the framework of critical path analysis (Ambegaokar et al., 1971; Pollak, 1972) developed within percolation theory (Shante and Kirkpatrick, 1971; Kesten, 1982; Stauffer and Aharony, 1994; Hunt and Ewing, 2009) to a network representation of the medium (Fatt, 1956) in order to quantify *all* distinct solute transport paths that can be connected through the system, and the fluid fluxes along those paths. The theoretical treatment to develop an entire solute arrival time distribution has been described in a series of existing publications (Hunt and Skinner, 2008, 2010; Hunt et al., 2011; Ghanbarian-Alavijeh et al., 2012). Knowing the topology of each system of paths (Sahimi, 1993; Lee et al., 1999; Sheppard et al., 1999) together with the associated fluid fluxes, made it possible to calculate the variations in the characteristic velocity along the path, and thus the total solute transport time (Hunt and Skinner, 2008, 2010; Hunt et al., 2011; Ghanbarian-Alavijeh et al., 2012). This treatment generated the solute arrival time distribution as a function of transport distance, and the results are in agreement with simulations (Liu et al., 2003). It was also applied to relevant studies including the prediction of silicate weathering rates and laboratory experiments on reactive solute transport (Hunt, 2015), the description of soil production as a function of time (Hunt and Ghanbarian, 2016), the evaluation of relevant importance of solute transport in limiting chemical weathering (Yu and Hunt, 2017a), and the examination of the steady-state assumption in certain landscape evolution models (Yu and Hunt, 2017b).

From percolation theory, the solute transport time, t, increases more rapidly than linearly with transport distance, x, in particular, as a power of x equal to the percolation backbone fractal dimensionality, D_b (Lee et al., 1999). For 3D flow in saturated media and for a wide range of conditions, $D_b = 1.87$ (Sheppard et al., 1999). Sahimi and Mukhopadhyay (1996) discuss limitations on this result arising from certain classes of long-range correlations in the pore space of the medium itself. Under 2D saturated conditions, such as a flow along a fracture plane, or along the walls of a cylindrical core, for example, $D_b = 1.64$. However, field observations (Glass et al., 1998) and experimental

results show that unsaturated conditions are common when flow is constrained to 2D surface, in which case that $D_b = 1.21$.

For unsaturated 3D flow, $D_b = 1.46$ for drying, but $D_b = 1.861$ for wetting conditions. In summary, using the exponent values given in (Sheppard et al., 1999):

$$t = t_0\left(\frac{x}{x_0}\right)^{1.46}\ \text{(3D drainage)}\quad t = t_0\left(\frac{x}{x_0}\right)^{1.87}\ \text{(3D saturated or imbibition)} \tag{1a}$$

$$t = t_0\left(\frac{x}{x_0}\right)^{1.64}\ \text{(2D saturated)}\quad t = t_0\left(\frac{x}{x_0}\right)^{1.22}\ \text{(2D unsaturated)} \tag{1b}$$

In the second expression in Eq. (1a), the distinction between 1.87 and 1.861 is neglected. Here we expect that 3D network connectivity is more common than 2D conditions, though perhaps is not universally applied. Also, since drying typically occurs due to plant transpiration, which involves either horizontal or upward moisture fluxes, we propose that any soil-formation processes occurring during drying can be neglected. Thus we can use the second expression in Eq. (1a) to describe solute transport distances.

Then we have, in the absence of soil erosion, the soil depth (x) as a function of time,

$$x = x_0\left(\frac{t}{t_0}\right)^{\frac{1}{1.87}} = x_0\left(\frac{t}{t_0}\right)^{0.53} \tag{2}$$

where x_0 is a typical particle size, x_0/t_0 is the net (deep) pore-scale infiltration rate. When these are all known for a given site, all adjustable parameters are eliminated in our model.

By taking the derivative of Eq. (2) one can derive the equation for soil production (bedrock-to-soil conversion, or weathered regolith creation),

$$\frac{dx}{dt} = R_s = \frac{1}{1.87}\frac{x_0}{t_0}\left(\frac{t}{t_0}\right)^{-0.47} = \frac{1}{1.87}\frac{I}{\phi}\left(\frac{x}{x_0}\right)^{-0.87} \tag{3}$$

In these expression, $(x_0/t_0) \equiv I/\phi$, I is the net infiltration rate, with $I = P - AET + run\text{-}on - run\text{-}off$ (P is precipitation, AET is the average evapotranspiration), and ϕ is the soil porosity (Hunt and Ghanbarian, 2016; Yu et al., 2017).

Adding the effects of an erosion rate, $E(t)$, generates the expression of rate of soil formation (net production),

$$\frac{dx}{dt} = R_s - E(t) = \frac{1}{1.87}\frac{I}{\phi}\left(\frac{x}{x_0}\right)^{-0.87} - E(t) \tag{4}$$

In principle such an equation can be solved numerically for $x(t)$ with an arbitrary erosion rate, but to date we have only addressed the case $E(t)$ being a constant, E. In addition, such an equation can form the basis for a landscape evolution model if horizontal transport of soil is incorporated, but our efforts in that area are still ongoing. Soil depth at time t can be calculated from the integration of Eq. (4),

$$x(t) = \int_0^t dt'(R_s - E) = \int_0^t \left(\frac{1}{1.87}\frac{I}{\phi}\left(\frac{x(t)}{x_0}\right)\right)^{-0.87} - E)dt' \tag{5}$$

Since the integral equation Eq. (5) does not have a closed-form analytical solution, soil depths are solved numerically.

3. Material and methods

Predicted soil depths using Eq. (5) were compared with published field data of alpine soils in the European Alps, Gongga Mountain, China, and Cordillera Vilcanota and Quelccaya Ice Cap region (CV-QIC), southeastern Peru, and soil developed on alluvial fan and terrace at Merced River, California (White et al., 1996; Goodman et al., 2001; He and Tang, 2008; Egli et al., 2014). Theoretical soil formation rates for alpine soils predicted using Eq. (4) were also compared with predictions using soil age-profile thickness (SAST) method done by Egli et al. (2014).

Soil at the Merced River terraces is dominated by sand ranging from 320 to 730 μm, and generates an average particle size of 530 μm. Particle size at Gongga Mountain, China has a much wider range from 65 to 2000 μm, so a geometric mean of 400 μm is taken as typical particle size. The papers of European Alps and CV-QIC, do not typically reference particle sizes, thus a typical particle size of 30 μm is used here. Silt is the middle particle size (geometric mean) class in soil classification schemes, and a middle silt particle size would thus, in the absence of any information regarding soil texture at a given site, be the best estimate for a median particle size. Silt particle sizes range from 2 to 63 μm (USGS), with a mean value of 32 μm. The individual arithmetic means of the three principal soil particle classes, clay, silt, and sand also generates a geometric mean of 30 μm. This is why a typical particle size of 30 μm would be a reasonable choice. Net infiltration rate I is calculated by considering not only precipitation, but also the water lost to both evapotranspiration and what runs off from surface flow (net run-off). Lvovitch (1973) estimates that, globally, AET = 65% of P, and 24% of P travels to streams by overland flow, leaving only 11% of P for deep infiltration. However, it is not always the case that the difference between run-on and run-of to be negative. For local sites, there can be a net gain of water from run-on less run-off. We assume a typical porosity of 0.4 (Hillel, 1998) to calculate the pore-scale infiltration rate. Relevant parameters used for each site for prediction are summarized in Table 1.

Run-off is 1.08 m/yr (Juen et al., 2007) with 60% from non-glacial melting (Kronenberg et al., 2016). Due to the lack of information of erosion rates at CV-QIC, values were estimated by considering the

Table 1
Precipitation (P), evapotranspiration (AET), *Run-off*, infiltration (I/ϕ), and erosion rate (E) used for predictions at the 4 study sites.

Site	x_0 (μm)	P (m/yr)	AET (m/yr)	*Run-off* (m/yr)	Upper bound		Lower bound	
					I/ϕ (m/yr)	E (m/Myr)	I/ϕ (m/yr)	E (m/Myr)
E. Alps[a]	30	1.1 to 2	0.27	1.06	1.675	42	–	–
GM[b]	400	1.95	0.7	0.52 to 0.99	1.825	2000	0.65	3000
MR[c]	530	0.31	0.26	0.01	0.1	7.5	0.1	20
QIC[d]	30	$I = 1.5$	–	0.65	2.13	100	2.13	200

[a] E. Alps = European Alps, P values are from Egli et al. (2014), AET from the evapotranspiration map of Europe on IMPACT2C web-atlas (IMPACT2C Web-Altas, accessed in Dec. 2016), *Run-off* value is from Wehren et al. (2010). Erosion rates (in tons/ha/yr) of European Alps were determined from an erosion map published by (Bosco et al., 2008), and converted to m/yr using the averaged soil density at each site.

[b] GM = Gongga Mountain, P value is from He and Tang (2008), AET is between 0.6 and 0.8 m/yr (Gao et al., 2007), mean value of 0.7 is taken here. Erosion rates range between 2000 and 3000 m/My (Ouimet et al., 2009). Given the fact that 80% of the total *Run-off* from Gongga Mountain comes from glacial melting (Cao, 1995), 20% of the range of *Run-off* rates from Lin and Wang (2010) was estimated as run-off lost from precipitation.

[c] MR = Merced River, *P, AET and Run-off* rates are from Cal-adapt website (Cal-adapt Website, accessed in June 2017). Erosion rates range from 7.5 to 20×10^{-6} m/yr (Graly et al., 2010).

[d] QIC = Cordillera Vilcanota and Quelccaya Ice Cap region, annual water accumulation (taken as infiltration rate here) is approximately 1.5 m/yr (Goodman et al., 2001).

denudation rates across eastern Bolivian Andes (19–22°S), and the denudation rates at northwestern Peruvian Andes. For northwestern Peruvian Andes, erosion rates range from 100 to 200 m/Myr (Abbühl et al., 2010). A comparable denudation rate of 150 m/Myr was generated from the geometric mean of denudation rates across eastern Bolivian Andes (Barnes and Pelletier, 2006). Therefore, 100 to 200 m/Myr might be reasonable for erosion rates at CV-QIC.

Given the wide range of parameters at the sites, upper and lower limits of predictions are calculated using the limits of individual parameters. Generally, upper bound is generated using highest I (obtained from highest P, and lowest AET and $Run\text{-}off$ values), with the lowest E, and vice versa for the lower bound. But for European Alps, since the lowest precipitation of 1.1 m results a negative I, only the upper bound is considered in this case.

4. Results

Comparison of theoretical soil depths predicted at European Alps, Gongga Mountain, CV-QIC, and Merced River from Eq. (5) and the observed soil depths are shown in Figs. 1–4. The majority of the observed soil depths are within predicted limits. In Fig. 1, the discrepancy is largest at small soil ages, especially at Morteratsch. Morteratsch itself shows a large scatter of soil depths at similar soil ages. Such scatter indicates a possible unstable environmental condition or that unusual climate events occurred at Morteratsch, which could affect the agreement, since uniform parameters such as a constant erosion rate are used to generate theoretical soil depths.

Agreement of observations and predictions improves as soil age increases, suggesting that our model performs better for older soils. Depths of younger soils (shallow soil depths) tend to be more vulnerable to external influences such as trampling from animals, changes of environmental conditions, and potential stochastic nature of erosion, including effects of landslides or avalanches. As the timescale increases, parameters of environmental conditions such as infiltration rate and erosion rate are getting closer to the historical average values, and the fluctuations caused by any short-term environmental changes will be buffered, and become less important. Thus as soil age increases, it is more predictable by the proposed model dealing with ideal circumstances with relative stable environmental conditions.

Soil formation rates predicted from Eq. (4) are compared with predictions using SAST methods (Egli et al., 2014). All of our results are generated using highest infiltration rate and smallest erosion rate for particular site to predict highest soil formation rates. Fig. 5 shows results for European Alps and Fig. 6 summarizes all 3 alpine soils at European Alps, Gongga Mountain, China, and CV-QIC, southeastern Peru. Soil formation rates predicted from the two methods agree well in time scale spanning 5 orders of magnitude, with an overall slightly lower predictions from our model, especially for CV-QIC. Moreover, by taking uniform parameters in our model, soils with the same age at particular site generate identical formation rate, while various rates are obtained from SAST method. From Figs. 5 and 6, most of our predictions pass within the scatter generated from SAST method at same soil ages. By neglecting any specific micro environmental conditions for individual soil samples, our model seems to generate an average soil formation rate among soils at same soil ages.

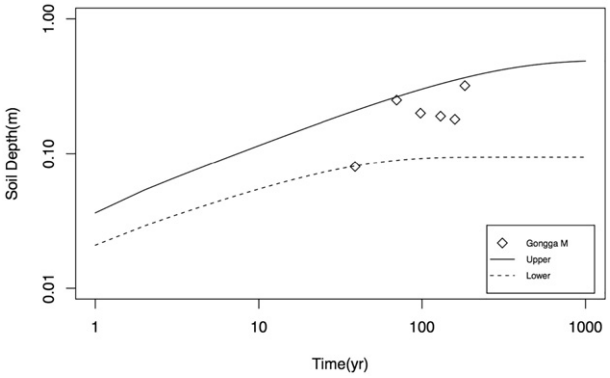

Fig. 2. Theoretical and observed soil depths at Gongga Mountain, China. Gongga M = Gongga Mountain.

5. Discussion

For all 4 study sites presented in this paper, majority of the field data are within the limits of maximum and minimum theoretical soil depths predicted from the proposed model (Eq. (5)). Upper and lower bounds of predictions are needed here due to the uncertainties and wide ranges of infiltration and erosion rates at each site. There are field results that lie outside the bounds of our predictions such as some soils at Morteratsch, European Alps. As a complicated process, soil formation is highly affected by environmental conditions, reflected by the high sensitivity of the soil-formation model to site parameters (particle size, infiltration rate and erosion rate). Thus specific site information is needed to generate exact predictions so that the accuracy of the model can be examined. However, the agreement between soil depths observed in the field and predictions across 4 different sites as well as the consistency of soil formation rates of alpine soils between our predictions and results from SAST methods (Egli et al., 2014) indicates possible implication of the proposed models in describing and predicting the formation of soil. By considering uniform parameters and constant erosion rates, the models presented in this paper deal with ideal circumstances with steady environmental conditions. Results show that the agreement between observation and prediction improves

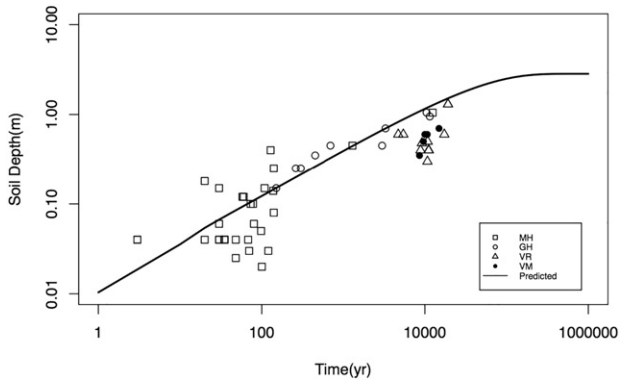

Fig. 1. Theoretical and observed soil depths at 4 sites in European Alps. MH = Morteratsch, GH = Gletsch, VR = Val di Rabbi, VM = Val Muilx.

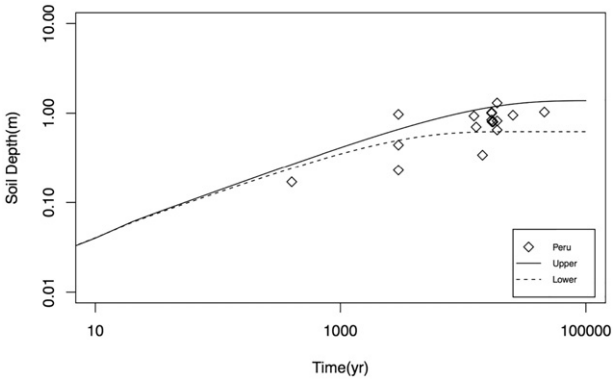

Fig. 3. Theoretical and observed soil depths at Cordillera Vilcanota and Quelccaya Ice Cap region, southeastern Peru.

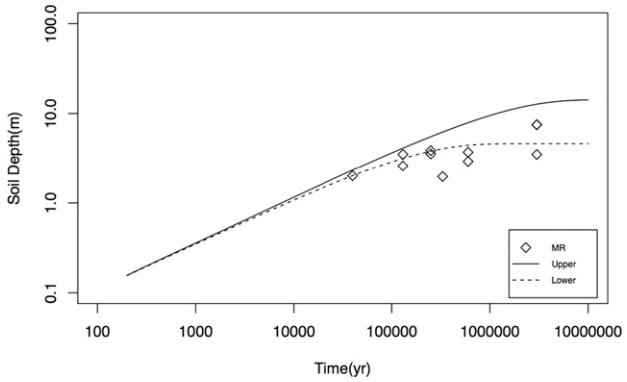

Fig. 4. Theoretical and observed soil depths at Merced River, California. MR = Merced River.

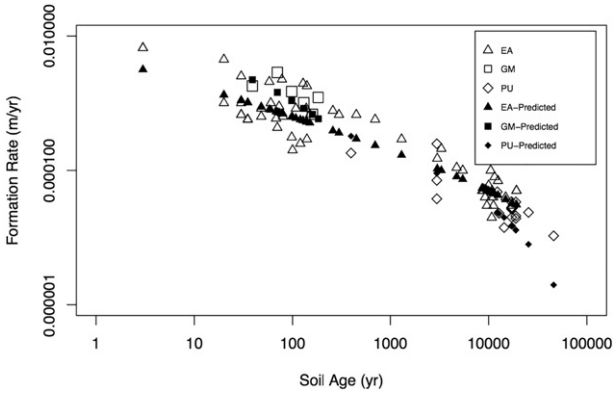

Fig. 6. Alpine soil formation rates predicted using proposed method (solids) and SAST method (open symbols, data published by Egli et al., 2014). EA = European Alps, GM = Gongga Mountain, China, PU = CV-QIC sites, Peru.

as time scale spans (at older soils). Possible reasons could be 1) younger soils with shallow soil depths are more vulnerable to external influences, 2) as timescales extends, any effects from short-term changes of the environment become less important. Therefore, large timescales allow soil to get closer to ideal circumstance, and make it more predictable by our theoretical model.

Landscape is sculpted by geomorphic processes such as soil production, soil erosion, among with other things. It has become clear that quantitative modeling of soil formation is critical to understanding landscape evolution. A number of landscape evolution models are built with adoptions of existing soil production models (Heimsath et al., 1997, 2000, 2001a, 2001b; Minasny and McBratney, 1999, 2001; Cohen et al., 2010; Liu et al., 2013). Since soil property strongly influence the direction and rates of geomorphic processes (Minasny and McBratney, 2006), soil production models also contribute studies in pedogensis models and the development of coupled geomorphological and pedogenic models (Minasny and McBratney, 2006; Welivitiya et al., 2016). Thus, the presented model in this paper will inform further study in evolution of soil and landforms. One of the applications is in examination of the steady-state assumption of certain soil development models (Yu and Hunt, 2017b), which is the simplest case in landform evolution.

The predicted soil evolution may also be relevant for Critical Zone Observatories (CZOs). In Fig. 7, we also show a comparison of our predictions using Eq. (5) with simulated results of soil evolution in Shale Hills CZO from a geomorphic-based analytical model (Liu et al., 2013). Simulation is obtained from the digitization of Fig. 9 (a) in Liu et al. (2013) (only the simulated results with initial soil depth equal to zero is digitized to match our initial condition). Value of annual infiltration rate is estimated from averaged recharge rates in 2009 and 2010 from the website of Shale Hills Critical Zone Observatory (CZO) (Susquehanna Shale Hills Critical Zone Observatory Website, accessed on July 14th, 2017). Erosion rate is about 15 m/My (Ma et al., 2010). To calculate the pore-scale infiltration rate, porosity is needed. Five series of soils are identified in the study site, and soil textures are mainly silt loam and silty-clay loam, with an averaged porosity around 0.52 down to B horizon (Lin, 2006). Kuntz et al. (2011) give a lower value of porosity of 0.45 for Ernest series. Silt loam has a d_{50} roughly 18 μm (Skaggs et al., 2001), which could be a reasonable estimation of the particle size. However, Lin (2010) discusses the importance of the soil structure, i.e., the soil aggregates, which act like much larger particles. Banwart et al. (2012) also emphasizes aggregate importance to flow paths at CZO sites including Shale Hills. Thus, particle size in Shale Hills could be larger than 18 μm. Typical particle size of soil (30 μm) might be a reasonable choice. Since our model is very sensitive to both of these two parameters, scenarios with various estimations of particle size and porosity are predicted and shown in Fig. 7. Although we don't generate precise agreement with stimulations from Liu et al. (2013), which itself has an RMSE of 0.394 m comparing with observed values, our predictions using 30 μm of particle size and 0.52 porosity are close to the stimulated results. However, without the knowledge of observed soil depths and information of soil properties, it is difficult to evaluate the precision of our model in predicting soils in the Shale Hills CZO.

6. Conclusion

Despite the discrepancy in soil depth at small soil ages which itself is highly affected by external influences and shows fluctuation and

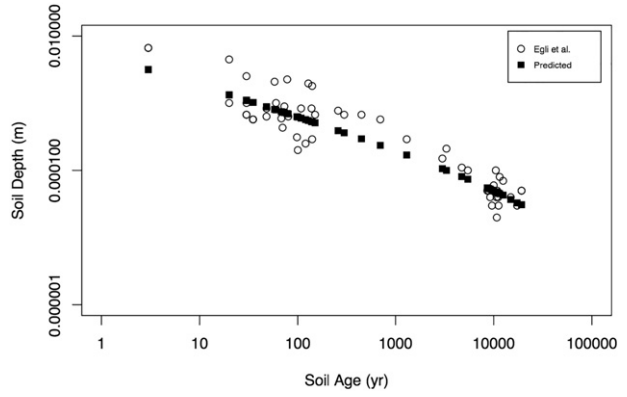

Fig. 5. Soil formation rates at European Alps. Squares are predicted rates using proposed model. Circles are published values by Egli et al. (2014) using SAST method.

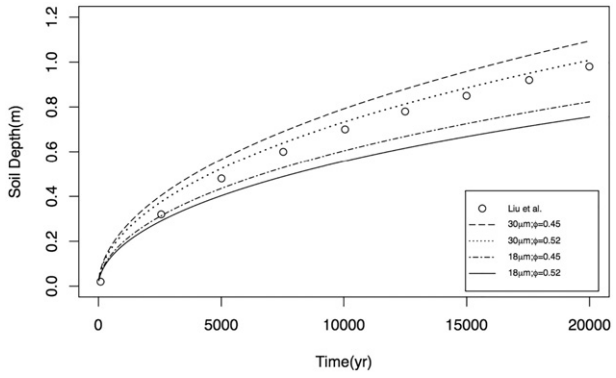

Fig. 7. Comparison of predictions to simulated results by Liu et al. (2013) of Shale Hills CZO. Lines represent predictions using various values of particle size (18 μm and 30 μm), and porosity (0.45 and 0.52).

inconsistency, the presented theoretical models derived from percolation theory can be used to describe and predict soil formation function in general. The accuracy improves as the timescale increases. However, additional information specific to each site is needed to further examine the accuracy of the models. If thorough testing confirms our initial results, our soil production model could be adopted for use with any landscape evolution model that accounts accurately for climate and vegetation conditions, provided some basic soil information is available and surface water routing is accounted for. Such an application in geomorphology may help in understanding of, for example, specific hillslope forms at smaller scales, improve the ability to predict regional denudation rates, and at the largest scales, generate results that help inform climate change predictions due to a more accurate accounting of chemical weathering and associated drawdown of atmospheric CO_2.

References

Abbühl, L.M., Norton, K.P., Schlunegger, F., Kracht, O., Aldahan, A., Rossnert, G., 2010. El Niño forcing on ^{10}Be-based surface denudation rates in northwestern Peruvian Andes? Geomorphology 123, 257–268.

Ambegaokar, V.N., Halperin, B.I., Langer, J.S., 1971. Hopping conductivity in disordered systems. Phys. Rev. B 4 (8):2612–2620. https://doi.org/10.1103/physrevb.4.2612.

Anderson, R.S., Anderson, S.P., 2010. Geomorphology: The Mechanics and Chemistry of Landscapes. Cambridge Press, New York.

Banwart, S., Bernasconi, S.M., Bloem, J., Blum, W.E.H., Brandao, M., Brantley, S., Chabaux, F., Duffy, C., Kram, P., Lair, G., Lundin, L., Nikolaidis, N., Novak, M., Panagos, P., Raagnarsdottin, K.V., Reynolds, B., Rousseva, S., de Ruiter, P., van Gaans, P., van Riemsdijk, W., White, T., Zhang, B., 2011. Soil processes and functions in critical zone observatories: hypotheses and experimental design. Vadose Zone J. 10 (3), 974.

Banwart, S., Menon, M., Bernasconi, S.M., Bloem, J., Blum, W.E.H., 2012. Soil processes and functions across an international network of critical zone observatories: introduction to experimental methods and initial results. Compt. Rendus Geosci. 344, 758–772.

Barnes, J.B., Pelletier, J.D., 2006. Latitudinal variation of denudation in the evolution of the Bolivian Andes. Am. J. Sci. 306, 1–31.

Benson, D., Wheatcraft, S., Meerschaert, M., 2000. Application of a fractional advection-dispersion equation. Water Resour. Res. 36, 1403–1412.

Berkowitz, B., Klafter, J., Metzler, R., Scher, H., 2002. Physical pictures of transport in heterogeneous media: advection-dispersion, random-walk, and fractional derivative formulations. Water Resour. Res. 38, 9-1–9-12.

Bijeljic, B., Muggeridge, A., Blunt, M., 2004. Pore-scale modeling of longitudinal dispersion. Water Resour. Res. 40. https://doi.org/10.1029/2004WR003567.

Bosco, C., Montanarella, L., Rusco, S., Oliveri, Panagos, P., 2008. Soil Erosion in the Alps according to IPCC B2 Scenario. Office of Official Publications of the European Communities, Luxembourg.

Burke, B., Heimsath, A., White, A., 2007. Coupling chemical weathering with soil production across soil-mantled landscapes. Earth Surf. Process. Landf. 32, 853–873.

Cal-adapt website. Available online. http://cal-adapt.org/data/tabular/ (accessed in June, 2017).

Cao, Z.T., 1995. The characteristics of glacier hydrology in the area of Gongga Mountain. J. Glaciol. Geocryol. 17, 73–83.

Carson, M.A., Kirkby, M.J., 1972. Hillslope Form and Process. Cambridge University Press, New York.

Cohen, S., Willgoose, G., Hancock, G., 2010. The mARM3D spatially distributed soil evolution model: three-dimensional model framework and analysis of hillslope and landform responses. J. Geophys. Res. Earth Surf. 115 (F4). https://doi.org/10.1029/2009JF001536.

Cushman, J., O' Malley, D., 2015. Fickian dispersion is anomalous. J. Hydrol. 531, 161–167.

Dixon, J., Heimsath, A., Kaste, J., Amundson, R., 2009. Climate-driven processes of hillslope weathering. Geology 37, 975–978.

Dokuchaev, V.V., 1967. Russian Chernozem, in, Selected works of V. V. Dokuchaev, Moscow, 1948, 1, 14–419. Israel Program for Scientific Translations Ltd. (for USDA-NSF), Publ. by S. Monson, Jerusalem (Transl. into English by N. Kaner). 1883/1948/1967.

Egli, M., Dahms, D., Norton, K., 2014. Soil formation rates on silicate parent material in alpine environments: different approaches–different results? Geoderma 213, 320–333.

Fatt, I., 1956. The network model of porous media. I. Capillary Pressure Characteristics. Petr. Trans. AIME. 207, 145–159.

Friend, J.A., 1992. Achieving soil sustainability. J. Soil Water Conserv. 47, 156–157.

Gao, G., Chen, D., Xu, C., Simelton, E., 2007. Trend of estimated actual evapotranspiration over China during 1960–2002. J. Geophys. Res.-Atmos. 112. https://doi.org/10.1029/2006JD008010/full.

Ghanbarian-Alavijeh, B., Skinner, T., Hunt, A., 2012. Saturation dependence of dispersion in porous media. Phys. Rev. E 86.

Glass, R.J., Nicholl, M., Yarrington, L., 1998. A modified invasion percolation model for low-capillary number immiscible displacements in horizontal rough-walled fractures: influence of local in-plane curvature. Water Resour. Res. 34, 3215–3234.

Goodman, Y.A., Rodbell, D.T., Seltzer, G.O., Mark, B.G., 2001. Subdivision of glacial deposits in Southeaster Peru based on pedogenic development and radiometric ages. Quat. Res. 56, 31–50.

Graly, A.J., Bierman, P.R., Reusser, L.J., Pavich, M.J., 2010. Meteori ^{10}Be in soil profiles—a global meta-analysis. Geochim. Cosmochim. Acta 74, 6814–6829.

He, L., Tang, Y., 2008. Soil development along primary succession sequences on moraines of Hailuogou Glacier, Gongga Mountain, Sichuan, China. Catena 72, 259–269.

Heimsath, A.M., Dietrich, W.E., Nishiizumi, K., Finkel, R.C., 1997. The soil production function and landscape equilibrium. Nature 388, 358–361.

Heimsath, A.M., Dietrich, W.E., Nishiizumi, K., Finkel, R.C., 1999. Cosmogenic nuclides, topography, and the spatial variation of soil depth. Geomorphology 27, 151–172.

Heimsath, A.M., Chappell, J., Dietrich, W.E., Nishiizumi, K., Finkel, R.C, 2000. Soil production on retreating escarpment in southeaster Australia. Geology 28, 787–790.

Heimsath, A.M., Chappell, J., Dietrich, W.E., Nishiizumi, K., Finkel, R.C., 2001a. Late Quaternary erosion in southeastern Australia: a field example using cosmogenic nuclides. Quat. Int. 83–85, 169–185.

Heimsath, A.M., Dietrich, W.E., Nishiizumi, K., Finkel, R.C., 2001b. Stochastic processes of soil production and transport: erosion rates, topographic variation and cosmogenic nuclides in the Oregon coast range. Earth Surf. Process. Landf. 26, 531–552.

Heimsath, A.M., Furbish, D.J., Dietrich, W.E., 2005. The illusion of diffusion: Field evidence for depth dependent sediment transport. Geology 33, 949–952.

Heimsath, A.M., Fink, D., Hancock, G.R, 2009. The 'humped' soil production function: eroding Arnhem Land, Australia. Earth Surf. Process. Landf 34:1674–1684. https://doi.org/10.1002/esp.1859.

Hillel, D., 1998. Environmental Soil Physics. Academic, San Diego.

Huggett, R., 1998. Soil chronosequences, soil development, and soil evolution: a critical review. Catena 32, 155–172.

Hunt, A.G., 2015. Predicting rates of weathering rind formation. Vadose Zone J. https://doi.org/10.2136/vzj2014.09.0123.

Hunt, A.G., 2016. Spatio-temporal scaling vegetation growth and soil production from percolation theory. Vadose Zone J. 15 (2). https://doi.org/10.2136/vzj2015.01.001.

Hunt, A.G., 2017. Spatio-temporal scaling of vegetation growth and soil production: explicit predictions. Vadose Zone J. 16. https://doi.org/10.2136/vzj2016.06.0055.

Hunt, A.G., Ewing, R.P., 2009. Lecture Notes in Physics. Percolation Theory for Flow in Porous Media. Springer, Berlin.

Hunt, A.G., Ghanbarian, B., 2016. Percolation theory for solute transport in porous media: geochemistry, geomorphology, and carbon cycling. Water Resour. Res. 52, 7444–7459.

Hunt, A.G., Skinner, T., 2008. Longitudinal dispersion of solutes in porous media solely by advection. Philos. Mag. 88, 2921–2944.

Hunt, A.G., Skinner, T.E., 2010. Incorporation of effects of diffusion into advection-mediated dispersion in porous media. J. Stat. Phys. 140 (3):544–564. https://doi.org/10.1007/s10955-010-9992-x.

Hunt, A.G., Yu, F., 2017. Use of constructal theory in modeling in the geosciences. In: Ghanbarian, Behzad, Hunt, Allen (Eds.), Fractals: Concepts and Applications in the Geosciences. CRC Press, Boca Raton Fl.

Hunt, A.G., Skinner, T., Ewing, R., Ghanbarian-Alavijeh, B., 2011. Dispersion of solutes in porous media. The European Physical Journal B 80, 411–432.

IMPACT2C Web-Altas, d. Evapotranspiration of Europehttps://www.atlas.impact2c.eu/en/climate/evapotranspiration/ (accessed on December 15th, 2016).

Jenny, H., 1941. Factors of Soil Formation: A System of Quantitative Pedology. Dover, N.Y.

Juen, I., Kaser, G., Georges, C., 2007. Modelling observed and futrue runoff from a glacierized tropical catchment (Cordillera Blanca, Perú). Glob. Planet. Chang. 59, 37–48.

Kesten, H., 1982. Percolation Theory for Mathematicians. 1982. Birkhauser, Boston, Mass. (423pp).

Krepysheva, N., Di Pietro, L., Néel, M.C., 2006. Space-fractional advection-diffusion and reflective boundary condition. Phys. Rev. E 73. https://doi.org/10.1103/PhysRevE.73.021104.

Kronenberg, M., Shauwecker, S., Huggel, C., Salzmann, N., Drenkhan, F., Frey, H., Giráldz, C., Gurgiser, W., Kaser, G., Juen, I., Suarez, Wl, Hernández, J.G., Sanmrtín, Ayros, E., Perry, B., Rohere, M., 2016. The projected precipitation reduction over the Central Andes may severely affect Peruvian glaciers and hydropower production. Energy Procedia 97, 270–277.

Kuntz, B., Rubin, S., Berkowitz, B., Singha, K., 2011. Quantifying solute transport at the Shale Hills Critical Zone Observatory. Vadose Zone J. 10, 843–857.

Lee, Y., Andrade, J., Buldyrev, S., Dokholyan, N., Havlin, S., King, P., Paul, G., Stanley, H., 1999. Traveling time and traveling length in critical percolation clusters. Phys. Rev. E 60, 3425–3428.

Lin, H., 2006. Temporal stability of soil moisture spatial pattern and subsurface preferential flow pathways in the Shale Hills catchment. Vadose Zone J. 5, 317–340.

Lin, H., 2010. Linking principles of soil formation and flow regimes. J. Hydrol. 393, 3–19.

Lin, Y., Wang, G.X., 2010. Scale effect on runoff in alpine mountain catchments on China's Gongga Mountain. Hydrol. Earth Syst. Sci. Discuss. 7, 2157–2186.

Liu, Z., Wang, X., Mao, P., Wu, Q., 2003. Tracer dispersion between two lines in two-dimensional percolation porous media. Chin. Phys. Lett. 20 (11):1969–1972. https://doi.org/10.1088/0256-307x/20/11/019.

Liu, J., Chen, X., Lin, H., Liu, H., Song, H., 2013. A simple geomorphic-based analytical model for predicting spatial distribution of soil thickness in headwater hillslopes and catchments. Water Resour. Res. 49, 7733–7746.

Lvovitch, M.I., 1973. The Global Water Balance: U.S. National Committee for the International Hydrological Decade. National Academy of Science Bulletin, pp. 28–42 no. 23.

Ma, L., Chabaux, F., Pelt, E., Blaes, E., Jin, L., Brantley, S., 2010. Regolith production rates calculated with uranium-series isotopes at Susquehanna/Shale Hills critical zone observatory. Earth Planet. Sci. Lett. 297, 211–225.

Margolin, G., Berkowitz, B., 2000. Application of continuous time random walks to transport in porous media. J. Phys. Chem. B 104, 3942–3947.

Meerschaert, M., Benson, D., Bäumer, B., 1999. Multidimensional advection and fractional dispersion. Phys. Rev. E 59, 5026–5028.

Minasny, B., Mcbratney, A.B., 1999. A rudimentary mechanistic model for soil production and landscape development. Geoderma 90, 3–21.

Minasny, B., Mcbratney, A.B., 2001. A rudimentary mechanistic model for soil formation and landscape development II: a two-demiensional model incorporating chemical weathering. Geoderma 103, 161–179.

Minasny, B., Mcbratney, A.B., 2006. Mechanistic soil-landscape modelling as an approach to developing pedogenetic classifications. Geoderma 133, 138–149.

Montgomery, D.R., Brandon, M.T., 2002. Topographic controls on erosion rates in tectonically mountain ranges. Earth Planet. Sci. Lett. 201, 481–489.

Ouimet, W.B., Whipple, K., Granger, D.E., 2009. Beyond threshold hillslopes: channel adjustment to base-level fall in tectonically active mountain ranges. Geology 37, 579–582.

Pachepsky, Y., Benson, D., Rawls, W., 2000. Simulating scale-dependent solute transport in soils with the fractional advective-dspersive equation. Soil Sci. Soc. Am. J. 64, 1234–1243.
Pollak, M., 1972. A percolation treatment of dc hopping conduction. J. Non-Cryst. Solids 11, 1–24.
Runge, E.C.A., 1973. Soil development sequences and energy models. Soil Sci. 113, 183–193.
Sahimi, M., 1993. Fractal and superdiffusive transport and hydrodynamic dispersion in heterogeneous porous media. Transp. Porous Media 13 (1):3–40. https://doi.org/10.1007/bf00613269.
Sahimi, M., Mukhopadhyay, S., 1996. Scaling properties of a percolation model with long-range correlations. Phys. Rev. E 54:3870. https://doi.org/10.1103/PhysRevE.54.3870.
Schaetzl, R.J., Schwenner, C., 2006. An application of the Runge "energy model" of soil development in Michigan's upper peninsula. Soil Sci. 171, 152–166.
Shante, V.K.S., Kirkpatrick, S., 1971. Introduction to percolation theory. Adv. Phys. 20 (85): 325–357. https://doi.org/10.1080/00018737100101261.
Sheppard, A., Knackstedt, M., Pinczewski, W., Sahimi, M., 1999. Invasion percolation: new algorithms and universality classes. J. Phys. A Math. Gen. 32, L521–L529.
Skaggs, T.H., Arya, L.M., Shouse, P.J., Mohanty, B., 2001. Estimating particle-size distribution from limited soil texture data. Soil Sci. Soc. Am. J. 65, 1038–1044.
Stauffer, D., Aharony, A., 1994. Introduction to Percolation Theory. 2nd ed. Taylor and Francis, London, UK.
Susquehanna Shale Hills Critical Zone Observatory Website, d. http://criticalzone.org/shale-hills/infrastructure/field-areas-shale-hills/ (accessed on July 14th).
Vladychenskiy, A.S., 2009. Genesis of Soils and Factors of the Soil Formation. In: Glazovsky, N., Zaltseva, N. (Eds.), Environment Structure and Function: Earth System. EOLSS Publications.
Wehren, B., Weingartner, R., Schädler, B., Viviroli, D., 2010. General characteristics of Alpine Waters. Alpine Waters 6, 17–58.
Welivitiya, W.D.D.P., Willgoose, G.R., Hancock, G.R., Cohen, S., 2016. Exploring the sensitivity on a soil area-slope-grading relationship to changes in process parameters using a pedogenesis model. Earth Surface Dynamics 4, 607–625.
White, A.F., Brantley, S.L., 2003. The effect of time on the weathering of silicate minerals: why do weathering rates differ in the laboratory and field? Chem. Geol. 202 (3–4), 479–506.
White, A.F., Blum, A.E., Schulz, M.S., Bullen, T.D., Harden, J.W., Peterson, M.L., 1996. Chemical weathering rates of a soil chronosequence on granitic alluvium: I. Quantification of mineralogical and surface area changes and calculation of primary silicate reaction rates. Geochim. Cosmochim. Acta 60 (14), 2533–2550.
Yu, F., Hunt, A.G., 2017a. Damköhler number input to transport-limited chemical weathering and soil production calculations. ACS Earth and Space Chemistry 1 (1), 30–38.
Yu, F., Hunt, A.G., 2017b. An examination of the steady-state assumption in soil development models with application to landscape evolution. Earth Surf. Process. Landf. https://doi.org/10.1002/esp.4209.
Yu, F., Faybishenko, B., Hunt, A.G., Ghanbarian, B., 2017. A simple model of the variability of soil depths. WaterSA 9 (7), 460.